Membrane and Water Treatment, *Vol. 11, No. 2 (2020) 151-158*
DOI: https://doi.org/10.12989/mwt.2020.11.2.151

Preparation, characterization of activated carbon fiber from luffa and its application in CVFCW for rainwater treatment

Sanjrani Manzoor Ahmed[1], Boxun Zhou[2], Heng Zhao[3], You Ping Zheng[4], Yue Wang[5] and Shibin Xia*[6]

School of Resources and Environmental Engineering, Wuhan University of Technology, Wuhan, P. R. China

(Received June 24, 2019, Revised January 28 2020, Accepted February 3, 2020)

Abstract. ACF preparation from different materials has been attached with great attention during these years. This study was conducted to prepare activated carbon fiber (ACF) from luffa through the processes i.e pre-treatment, pre-oxidation and carbonization activation. Besides, this study also characterizes the ACF and its effect, i.e effect of pre-oxidation time and temperature also activation time and temperature on the compressive strength of ACF were investigated. The results from SEM, BET, FTIR and XRD show that the ACF is very efficient. The products under the optimum conditions had a specific surface area of 478.441 m2 /g with an average pore diameter of 3.783nm, and a pore volume of 0.193 cm3 /g. The surface of the luffa fiber is degummed and exposed, which is beneficial to the subsequent process and the increase of product properties. The compressive strength of HP-ACF was prepared under the optimum conditions, which can reach 0.2461 MPa. ACF is rich in micro-pores and has a good application prospect in the field of environmental protection.

Keywords: Luffa, Activated carbon fibers, Surface oxidation, Pyrolysis, Porous structure

Graphical Abstract

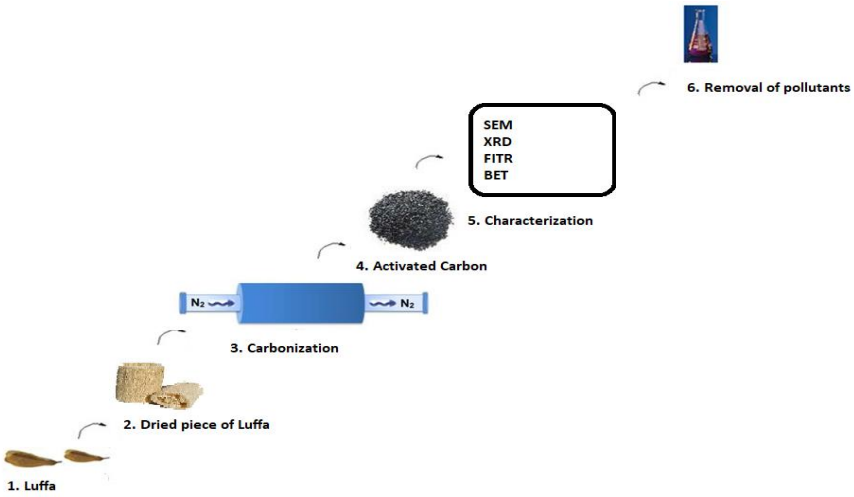

1. Introduction

Nowadays, water problems are being solved through different techniques worldwide. In recent years, there are many methods being used to remove pollutants from contaminated water, such as chemical oxidation, photocatalytic advanced oxidation and biological degradation. However, the use of ACF in wetlands technology has aroused the great interest among researchers. With the help of activation with some gas or chemical reagent, activated carbon fibers (ACFs) are prepared, due to their large specific surface area and with large amounts of well-defined porous structures, they are being widely utilized in several fields, such as purification, separation, electronic materials, catalysts (Teow *et al.* 2017, Jian Lin and Guangjie Zhao 2016, Garfi *et al.* 2012, Liu *et al.* 2009, Sanjrani MA *et al.* 2019a). Several studies have found that addition of ACF in wetlands have demonstrated promising results. Though wetland technology has been boosted with the addition of ACF but selection of biomass for preparing ACF is also important because various mechanisms are playing corresponding roles to control the heavy metals removal from aqueous solutions using ACF, including precipitation, complexation, ion exchange, electrostatic interaction (chemisorption), and physical sorption. In

*Corresponding author, Professor
E-mail: xiashibin@126.com
[a] Ph.D. Student
E-mail: manzoor.geo@gmail.com

ISSN: 2005-8624 (Print), 2092-7037 (Online)

addition, ACF and biochar are widely used as an adsorbent because of the good adsorption performance resulting from the complicated surface structure (A. Eliyas *et al.* 2019, Ouyang *et al.* 2016, Hu *et al.* 2011, Qian *et al.* 2004, Liu Zhenyu, and Zheng Jingtang 2010). Li *et al.* (2010) reported that the surface properties of ACF could affect the adsorption capacities of pollutants. El Qada *et al.* (2008) also demonstrated that the adsorption process was influenced by the surface area and the distribution of pores and pore volumes, which have a greater affinity for metals given that metallic ions can be physically sorbed onto the char surface and retained within the pores (Kumar *et al.* 2011, Xiao 2012, Zhengfang 2005). There are many ACF surfaces having been negatively charged and can sorb metals positively charged through electrostatic attractions, ligands specificity and various functional groups on ACF can also interact with various heavy metals by forming complexities (Dong et at 2011, C. Orhaa *et al.* 2018, Sanjrani MA *et al.* 2019b, El Qada et at 2008). Different ACF gives different results in constructed wetlands. During last couple of years, ACF fibers derived from luffa Cylindrica have emerged as promising adsorbent materials for harmful heavy metal ions and other pollutants. Based on their unique vascular structure, they exhibit a large surface area and thus high capability for the adsorption of metal ions (Li 2012, Ioanna *et al.* 2017, Li, Y *et al.* 2010). However, there are still gaps to be answered. This study mainly focuses on preparing, characterizing and providing the information of removal efficiency of ACF (prepared from luffa) by orthogonal test method. Influence factors of ACF, determination of porosity, determination of yield, determination of compressive strength was also investigated in this study. After preparation of ACF, It was added in composite vertical flow constructed wetland for rainwater treatment. Results show that after the pretreatment of Wuhan City rainwater by a Composite Vertical Flow Constructed Wetlands unit, the content of total nitrogen, Ammonia nitrogen and total Phosphorus decreased significantly, while the removal rate of COD was relatively low. More investigation are required to improve the quality of ACF.

2. Materials and methods

2.1 Materials and chemicals

Material was produced by Henan luohe hua hui co LTD. Afterwards, it was washed repeatedly with distilled water and dried in the air. All chemicals used during the preparation phase were of analytically better; standard solutions.

2.2 Preparation of ACF

Pretreatment for cylindrical luffa was conducted; firstly, the material needs to be soaked in 2% sodium hydroxide solution for 24 hours. After filtering, luffa materials were repeatedly washed to neutral and were dried in oven at 105 °C for 12 hours to obtain cylindrical alkali treated luffa materials, which were cut into small pieces with the size of 2×2 cm. For modification, alkali-treated dried luffa was put into water-soluble phenolic resin with a solid content of 35% for more than 24 hours till being fully immersed and then dried at 105 °C for 12 hours after being drained at the room temperature. Carbon activation process was followed; the impregnated luffa was put into the high temperature resistance furnace, pre-oxidized it for 2 hours at 200 °C and then put into the high temperature resistance furnace for carbonization activation. Protective gas N_2 into the high temperature resistance furnace was introduced at the controlled rate flow 0.5-0.8L/min. In addition, the activation temperature was 850 °C. The ACF was finally obtained. The obtained product was immersed in 1 mol of HCl solution for 120 min to remove residual ash in the product. The product was subsequently washed to neutral with hot deionized water, and dried in an oven at 105 °C for 12 h to obtain ACF, and then stored for future use

2.3 Physicochemical characterization of ACF

2.3.1 Scanning Electronic Microscopy (SEM)

A scanning electron microscope (SEM) (MIRA3, TESCAN) was used to measure surface morphology and also the micro metrics of the ACF.

2.3.2 Fourier Transform Infrared Spectroscopy (FTIR)

Fourier transform infrared spectrometer (Tensor27, Bruker Company, Germany) in the range 400–4000 cm−1 at a resolution of 2 cm−1 was applied for the qualitatively analysis for the functional groups.

Other measurements were also done with proper tools and techniques.

- The ACF surface area was determined by using an ASAP-2020 surface area analyzer (Micromeritics Instrument Corporation, USA).
- Vario Elemental Analyzer (Elementar Company, Germany) was used to record the elemental analysis of the ACF.
- XRD pattern of the original luffa and sample 0 were determined.
- The microstructure of ACF is a series of indicators, such as the nitrogen adsorption desorption curve, specific surface area and average pore diameter obtained by BET detection.

2.3.3 Determination of porosity

GB9966.3-88 was used as the reference for the evaluation of the natural facing stone volume density, true density, true porosity, porosity, water absorption test method.

2.3.4 Determination of Yield

Yield (η) here refers to the percentage of the final product to the quality of fibers (soaked in phenolic resin), which is used to measure the index of the preparation of the activated carbon fibers from modified fibers by the carbonization activation method. The raw material fibers were modified by phenolic resin solution, and dried to obtain a mass. Yield was calculated as raw material mass of m1. After processing the carbonization and activation, the mass of ACF was considered as m, and the yield of ACF was as follows:

$$\eta = \frac{m}{m_1} * 100\% \quad (1)$$

2.3.5 Determination of compressive strength

The mechanical properties of high strength biomass activated carbon fibers were tested by the impact tester50J/XJD-50. The maximum pressure was measured when the sample was broken. Afterwards, the compressive strength of the sample was calculated from the known area of the stress surface.

2.3.6 Influence factors of ACF

The influencing factors of ACF were selected according to the relevant data, i.e heating rate, pre-oxidation temperature, pre-oxidation time, activation temperature and activation time (see the table S4), which had great influence on the yield and performance of ACF. There were four levels being selected for each factor and L16 (45) orthogonal design table was used to carry out the experiment. The index range of each factor in the orthogonal experiment was determined by the orthogonal table according to the pre-experiment, the factor level table of which is demonstrated in table S4.

3. Results and discussion

3.1 Analysis of orthogonal test results

The data was analyzed through range analysis while the influenced degree of each factor on the ACF porosity was activated temperature > heating rate> pre-oxidation temperature > activation time > pre-oxidation time (see to table 1-2). The data was also analyzed to evaluate the influence degree of each factor on the adsorption performance of ACF, which was activated by temperature > heating rate > pre-oxidation temperature > pre-oxidation time > activation time (see table 1-2). Here effect of different parameters on the performance of ACF is given in Fig 1.

According to the weight of the porosity and compressive strength in the test, a comprehensive analysis was carried out, in which the porosity accounts for 60% while the compressive strength accounts for 40%. The range analysis (see table 1-2) determined that the factors affecting ACF performance are ranked as follows: activation temperature > heating rate > pre-oxidation temperature > activation time > pre-oxidation time. Compared with the impact of the same factor mean value, the best combination process for ACF preparation should be A3B3C4D4E4. The heating rate was 8 °C/min and the pre-oxidation temperature was 220 °C. The pre-oxidation time was 150 min.

The corresponding activation temperature was 800 °C while the activation time was 90 min. The product under the process was named as sample 0 and the HP-ACF has a bulk volume of 6*30*π*52=14130 cm3, which was prepared by this scheme to be used as a filler in a subsequent water treatment test. This product has been used for rainwater treatment and further it will be used for removal of antibiotic in composite vertical flow constructed wetland.

Table 2 Comprehensive Analysis Table

	Factor				
	A	B	C	D	E
	Heating rate	Pre-oxidation temperature	Pre-oxidation time	Activation temperature	Activation time
Mean 1	40.31	39.49	39.63	36.18	41.01
Mean 2	40.83	40.83	40.28	38.42	40.47
Mean3	42.69	42.04	40.84	43.11	39.66
Mean4	38.76	40.29	41.89	45.39	41.98
Range	3.93	2.55	2.26	9.21	2.32
Influence level	2	3	5	1	4

Table 1 Orthogonal test results

Test group number	Heating rate / (°C/min)	Pre-oxidation temperature /°C	Pre-oxidation time/min	Activation temperature / °C	Activation time/ min	Porosity/%	Yield/%	Compressive strength/ 104pa
1	6	180	60	500	60	50.6	49.79	8.463
2	6	200	90	600	70	52.4	53.00	14.973
3	6	220	120	700	80	61.8	51.74	15.012
4	6	240	150	800	90	64.0	46.81	21.457
5	7	180	90	700	90	60.2	47.92	16.130
6	7	200	60	800	80	58.4	45.92	20.467
7	7	220	150	500	70	55.3	53.95	13.969
8	7	240	120	600	60	54.2	49.03	15.549
9	8	180	120	800	70	63.4	42.76	19.307
10	8	200	150	700	60	62.8	48.02	23.010
11	8	220	60	600	90	59.7	49.58	14.556
12	8	240	90	500	80	52.8	54.33	11.930
13	9	180	150	600	80	51.8	51.95	12.015
14	9	200	120	500	90	53.2	47.59	9.636
15	9	220	90	800	60	64.3	43.71	15.216
16	9	240	60	700	70	54.8	36.26	17.564

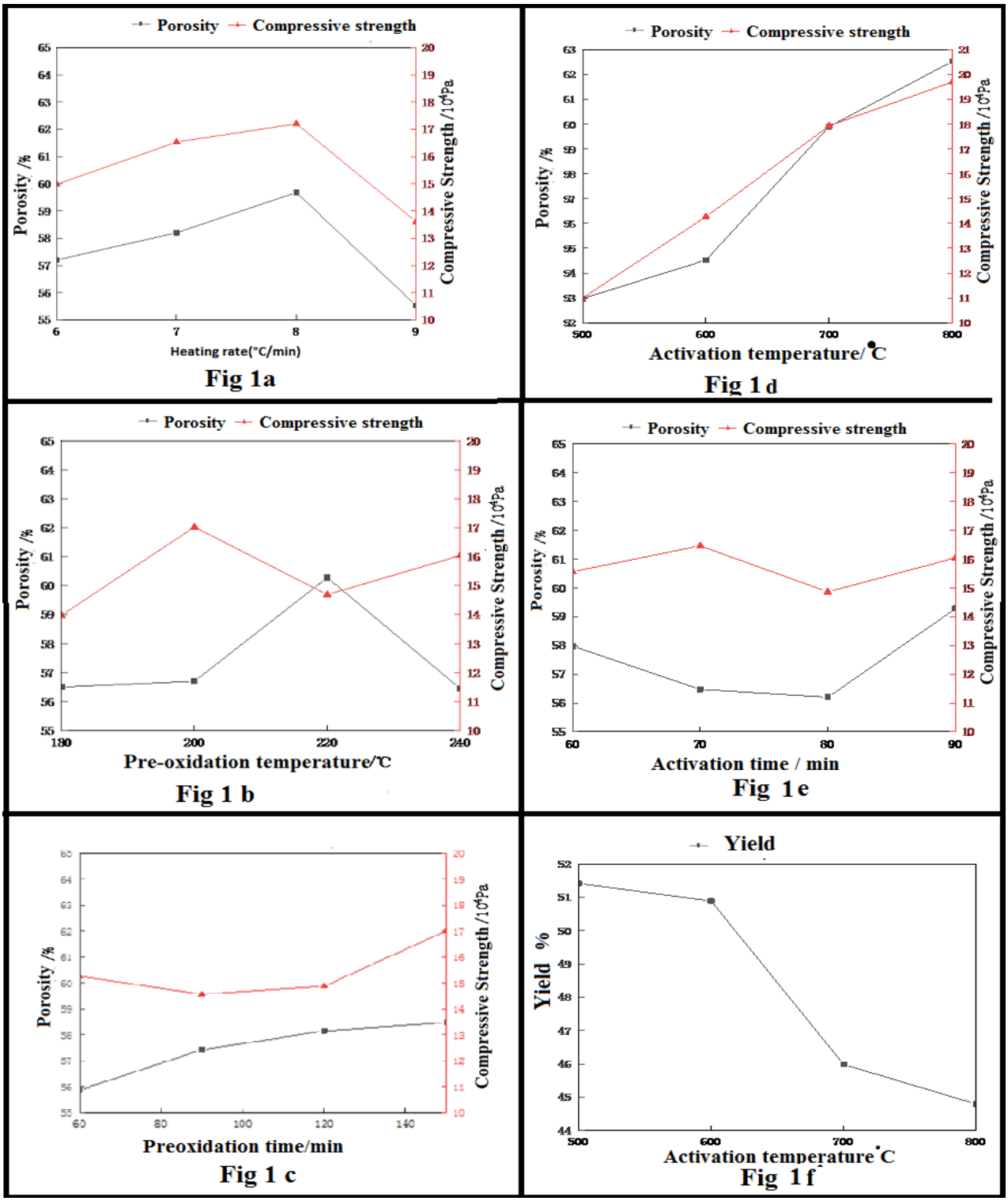

Fig. 1 Effect of different parameters on the performance of ACF

3.2 Scanning electron microscope

The surface topography of the luffa fiber sample before and after alkali (NaOH) treatment is shown in Figures 2a (Raw materials) and 2b (Raw materials after alkali treatment). As it can be seen from the figure, the surface of the raw material is smooth and flat. The surface contains a very thick wax. A large number of grooves are formed on the surface of the luffa fiber after the alkali treatment. After the treatment with NaOH, a large amount of particulate matter appears on the surface of the raw material because the surface of the raw material is degummed with NaOH. Besides, the lignin and hemicellulose are removed, so that the surface is exposed, which is advantageous for the subsequent carbonization activation processes.

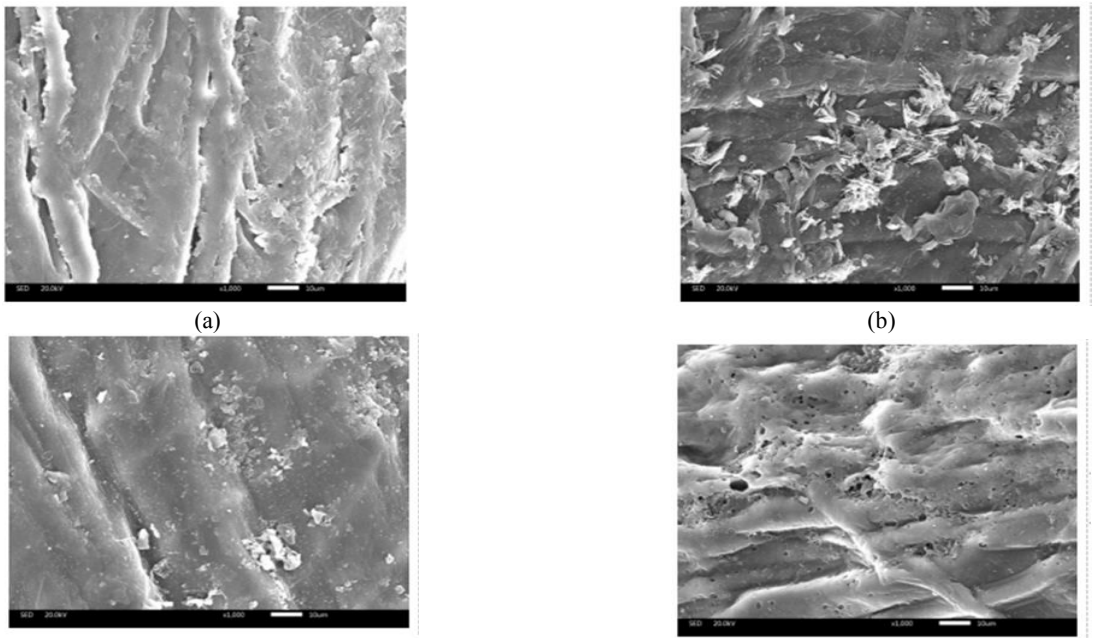

(a) (b) (c) (d)

Fig. 2 SEM Results

The surface topographies of Sample 1 and Sample 0 under optimal conditions were observed by SEM, (see Figures 2b, 2c (Sample 1 product)). It can be seen from the figure that the surface of the sample 1 is smooth and non-porous. I n contrast, the surface of the sample 0 is rough and porous (Fig 2d (Sample 0 product)).

This is because the activation temperature (500 °C) of the sample 1 is relatively low, the heating rate (6 °C / min) is relatively slow, the activation temperature of the sample 0 is 800 ° C, and the heating rate is 8 °C / min.

3.3 Microstructure of ACF

The microstructure of ACF is a series of indicators, such as the nitrogen adsorption desorption curve, specific surface area and average pore diameter obtained by BET detection. Fig. 3a: Nitrogen adsorption-desorption curve of Sample 1 and Figure 3b Nitrogen adsorption desorption curve of sample 9 and Figure 3c, Nitrogen adsorption desorption curve of sample 0. As shown in Figures 3a, 3b, and 3c, the nitrogen adsorption desorption curves of samples 0, 1, and 9 are similar while the adsorption and desorption curves are basically coincident.The ends are slightly upturned, all of which belong to the IUPAC (International Union of Pure and Applied Chemistry) classification of the adsorption isotherm.

The material properties belonging to the isotherm are mainly micropores and the pore size is narrow. It can be seen from Table S3 that as the activation temperature increases, the specific surface area also increases. This is because at the high temperature, the volatile component of the luffa is more volatile than the low temperature, which can lead ot the large internal space of luffa. Under the etching action of the volatile matter, the surface of the luffa also forms pores. Therefore, the pore volume and the average aperture are also increased.

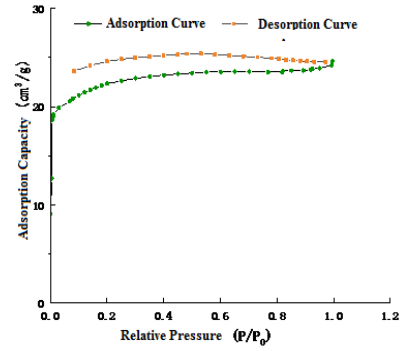

(a)

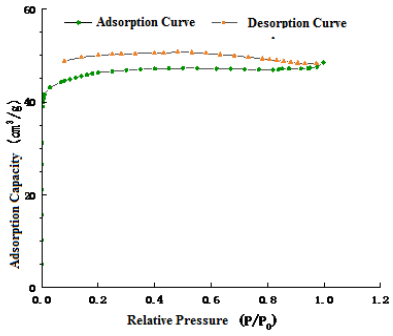

(b)

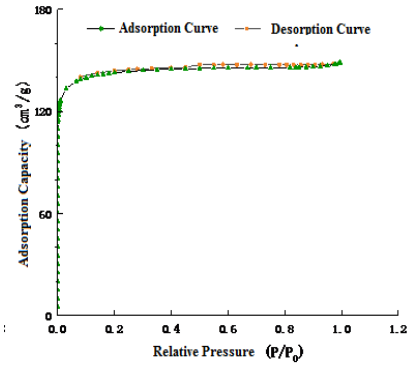

(c)

Fig. 3 Microstructure of ACF

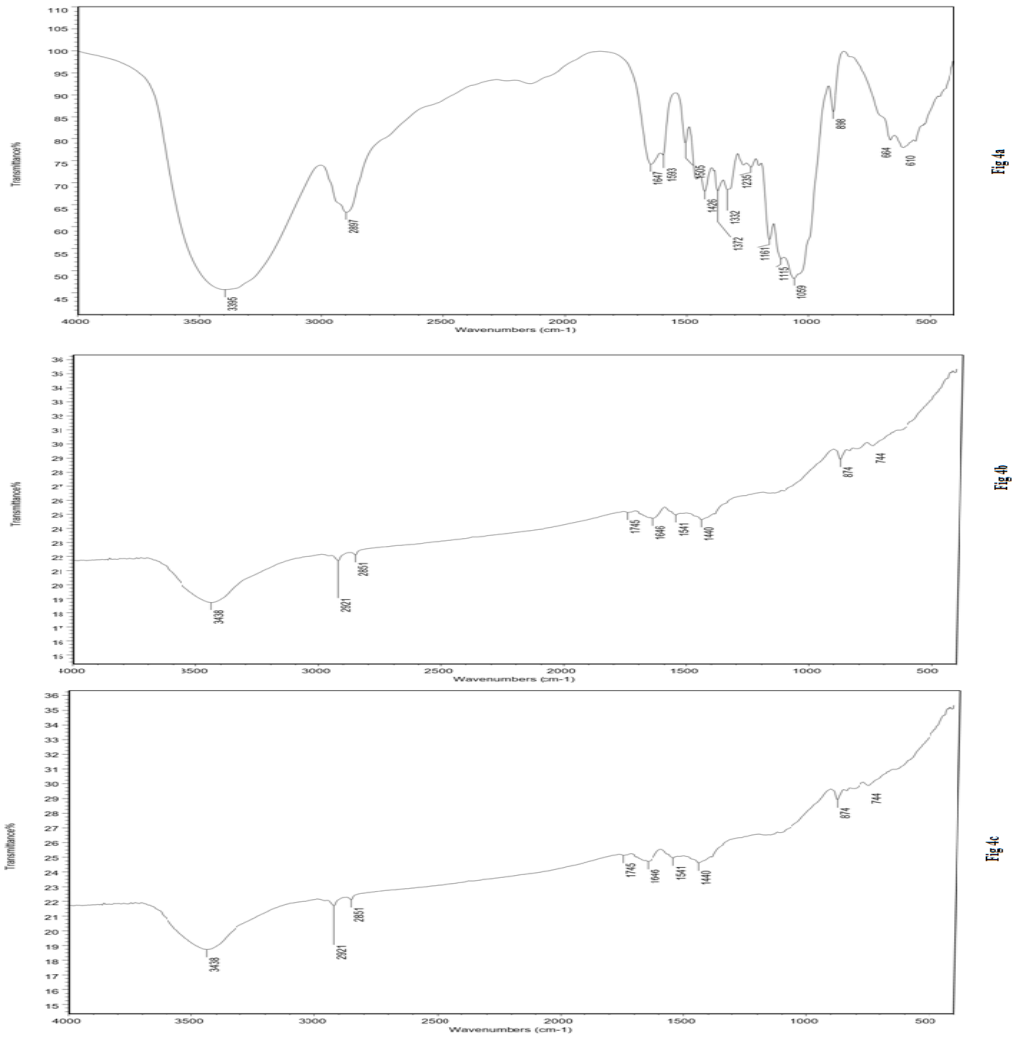

Fig. 4 Fourier Infrared Spectroscopy

3.4 Fourier infrared spectroscopy

FITR is mainly used to determine the qualitative and quantitative analysis of surface groups of samples. Figure 4a demonstrates the original Luffa FITR while Figure 4b demonstrates sample 1 FITR and Figure 4c demonstrates sample 0 FITR. Figure 4a shows the FITR diagram of the original luffa. It can be seen that the original luffa has more functional groups and complex compositions. Comparing Fig. 4b with Fig. 4c, it is found that most of the components in the luffa have been removed from the product by the reaction after the treatment and the shapes are very similar. Generally speaking, the absorption peaks of product ACF at 3442 cm-1 may be the stretching vibration peaks of O-H hydroxyl group, while those at 1637 cm-1 and 1560 cm-1 may be caused by the stretching vibration of adsorbed water, C=C on the framework of aromatic rings and C=O.

3.5 X-ray diffraction

The XRD pattern of the original luffa and sample 0 has been shown in figure 5. It can be seen from the figure that the luffa and its ACF products are both amorphous and have broad diffraction peaks. The absence of the original luffa in sample 0 indicates that the diffraction peaks of cellulose and carbohydrate molecules at 2θ=15°. This implies that they destroyed the substances in the luffa during the preparation process and the luffa undergoes carbon rearrangement at 2θ=44°. The diffraction peaks that are not found in the luffa may be caused by the pyrolysis of the phenolic resin.

3.6 ACF performance characterization

The performance characterization of ACF is mainly divided into two parts. One is the characterization of the adsorption performance of ACF while the second part is the characterization of the compressive strength of ACF. The performance of ACF mainly depends on the physicochemical properties of its surface. The surface physical properties include the surface physical form of activated carbon fiber and the pore distribution and specific surface area of activated carbon fiber surface. The surface chemical properties of ACF mainly refer to its surface group and crystal structure. With regard to the other natures, compressive strength of activated carbon fibers mainly depends on the internal and surface defects of activated carbon fibers (Li X.B 2012). In this experiment, the surface morphology of luffa fibers and ACF was characterized by

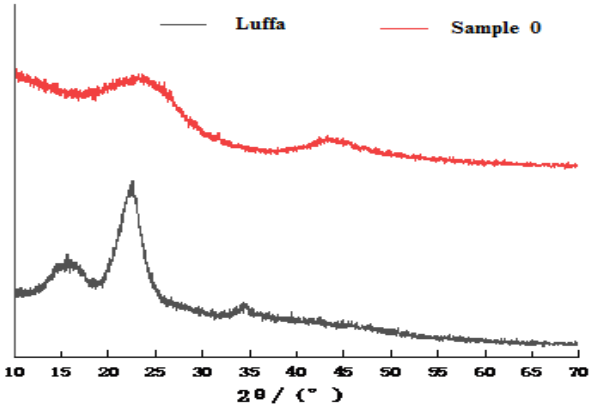

Fig. 5 XRD pattern of original luffa and sample 0

scanning electron microscopy (SEM) while the pore distribution of luffa surface was characterized by low temperature adsorption-desorption curve of nitrogen. X-ray diffraction (XRD) was used to characterize luffa fibers; the composition of ACF, the structural morphology of the molecule and the internal atoms. Fourier transform infrared spectroscopy (FTIR) was used to characterize the surface groups of the luffa fibers and ACF. The mechanical properties of the ACF were tested for its compressive strength using an impact tester model 50J/XJJD-50. It also tested the maximum pressure at which the sample is broken. Afterwards, the compressive strength of the sample is calculated from the known area of the stressed surface.

4. Application of prepared ACF

After successfully preparations, ACF was characterized with different techniques and found to be useful. It was added in composite vertical flow constructed wetland. The system was used to treat rain water. Result shows that addition of ACF can improve the efficiency of CWs for water treatment. Results is given in table no. 3.

Table 3 Results from composite vertical flow constructed wetlands

Total nitrogen %	Ammonia nitrogen %	Total phosphorus %	COD (cr) %
83.44	64.47	55.325	32.68
80.195	62.535	52.155	27.19
75.48	59.12	50.875	25

5. Conclusion

The process was evaluated by orthogonal test, the impact of the influencing factors and the characterization of the product. The results are as follows:

(1) The optimum combination process for ACF preparation should be conducted with a heating rate of 8 °C / min, a pre-oxidation temperature of 220 °C, a pre-oxidation time of 150 min, an activation temperature of 800 °C, and an activation time of 90 min.

(2) SEM results show that in the alkali treatment, the surface of the luffa fiber is degummed and exposed, which is beneficial to the subsequent process and the increase of product properties.

(3) The BET results indicate that the luffa itself and its products are all type I adsorption isotherms, which are characterized by micropores and narrow pore size. The products under the optimum conditions had a specific surface area of 478.441 m2 /g with an average pore diameter of 3.783nm, and a pore volume of 0.193 cm3 /g.

(4) FTIR showed that the surface of ACF prepared by this process contained hydroxyl and carboxyl groups and the internal structure was converted into aromatic ring structure.

(5) XRD analysis showed that the composition of the fibers was destroyed and the interior was rearranged after the process conditions. Finally, the luffa fiber was decomposed into amorphous carbon while the phenolic resin was decomposed into glass carbon.

(6) The compressive strength of ACF is tested by universal testing machine. The activation temperature is the most important factor affecting the compressive strength of ACF. The compressive strength of HP-ACF was prepared under the optimum conditions, which can reach 0.2461 MPa.

Therefore, it is recommended that deep analysis are needed. This ACF can work well, if preparation methods are carefully followed. Product can be more efficient and can be utilized for solving environmental issues.

Acknowledgements

This research was supported by the Demonstration of Integrated Management of Rocky Desertification and Enhancement of Ecological Service Function in Karst Peak-cluster Depression (grant no.:2016YFC0502400).

References

Dong, X.L., Ma, L.N.Q. and Li, Y.C. (2011), "Characteristics and mechanisms of hexavalent chromium removal by biochar from sugar beet tailing", *J. Hazardous Mater.*, **190**, 909-915. https://doi.org/10.1016/j.jhazmat.2011.04.008.

El Qada, E.N., Allen, S.J. and Walker, G.M. (2008), "Adsorption of basic dyes from aqueous solution onto activated carbons", *Chem. Eng. J.*, **135**, 174–184. https://doi.org/10.1016/j.cej.2007.02.023

Eliyas, S., Dimitrov, L., Stoyanova, E. and Fabian, M. (2019), "Synthesis and Properties of Binary V2O3 + TiO_2 Photocatalytic Materials for Wastewater and Air Decontamination", *J. Environ. Protection Ecology*, **20**(1), 265–275.

Fu, Z. (2005), "Preparation of polyacrylonitrile-based hollow activated carbon fiber and its hydrogen storage performance", Ph.D. Dissertation, Donghua University. (Translated)

Garfí, M., Pedescoll, A., Bécares, E., Hijosa-Valsero, M., Sidrach-Cardona, R. and García, J. (2012), "Effect of climatic conditions, season and wastewater quality on contaminant removal efficiency of two experimental constructed wetlands in different regions of Spain", *Sci. Total Environ.*, **437**, 61–67. https://doi.org/10.1016/j.scitotenv.2012.07.087.

Haan, T. Y., Shah, M., Chun, H. K. and Mohammad, A. W. (2018), "A study on membrane technology for surface water treatment:

Synthesis, characterization and performance test", *Membr. Water Treat.*, **9**(2), 69-77. https://doi.org/10.12989/mwt.2018.9.2.069

Hu, Y., Xia, J. and Li, J. (2011), "Effects of Different Carbon Additives on Strength and Adsorption Properties of Bulk Activated Carbon", *Carbon*, **30**(4), 1-3.

Kumar, S., Loganathan, V.A., Gupta, R.B. and Barnett, M.O. (2011), "An Assessment of U(VI) removal from groundwater using biochar produced from hydrothermal carbonization", *J. Environ. Manage.*, **92**, 2504-2512. https://doi.org/10.1016/j.jenvman.2011.05.013

Li, X. (2012), "Preparation and application of high performance viscose-based activated carbon fiber", Ph.D. Dissertation, Dalian University of Technology.

Li, Y., Du, Q., Wang, X., Zhang, P., Wang, D., Wang, Z. and Xia, Y. (2010), "Removal of lead from aqueous solution by activated carbon prepared from Enteromorpha prolifera by zinc chloride activation", *J. Hazard. Mater.*, **183**, 583–589. https://doi.org/10.1016/j.jhazmat.2010.07.063.

Liatsou, I., Pashalidis, I., Oezaslan, M. and Dosche, C. (2017), "Surface characterization of oxidized biochar fibers derived from Luffa Cylindrica and lanthanide binding", *J. Environ. Chem. Eng.*, https://doi.org/10.1016/j.jece.2017.07.040

Lin, J. and Zhao, G. (2016), "Preparation and Characterization of High Surface Area Activated Carbon Fibers from Lignin", *Polymers*, **8**, 369. https://doi.org/10.3390/polym8100369.

Liu, D., Ge, Y., Chang, J., Peng, C., Gu, B., Chan, G. Y. and Wu, X. (2009), "Constructed wetlands in china: recent developments and future challenges", *Front. Ecol. Environ.*, **7**, 261–268. https://doi.org/10.1890/070110.

Liu, Z. and Zheng, J. (2001), "Study on Nitrogen Adsorption of PAN-based Activated Carbon Fibers", *Acta Phys. Sinica*, **17**(7), 594-599.

Orhaa, C., Lazaua, C., Podeb, R. and Maneab, F. (2018), "Simultaneous removal of humic acid and arsenic(iii) from drinking water using tio2-powdered activated carbon", *J. Environ. Protect. Ecology*, **19**(1), 39–47.

Ouyang, W., Zhao, X.C., Tysklind, M. and Hao, F.H. (2016), "Typical agricultural diffuse herbicide sorption with agricultural waste-derived biochars amended soil of high organic matter content", *Water Res.*, **92**, 156–163. https://doi.org/10.1016/j.watres.2016.01.055.

Qian, J.M., Wang, J., Jin, Z. (2004), "Study on Preparation of Wood Ceramics from Eucalyptus Wood Powder and Phenolic Resin", *J. Inorganic Mater.*, **19**(2), 335-341. (Translated)

Sanjrani, M.A., Zhou, B., Zhao, H., Bhutto, S.A., Muneer, A.S. and Xia, S.B. (2019a), "Arsenic contaminated groundwater in china and its treatment options, A review", *Appl. Ecology Environ. Res.* **17**(2), 1655-1683. http://dx.doi.org/10.15666/aeer/1702_16551683.

Sanjrani, M.A., Zhou, B., Zhao, H., Zheng, Y. P., Wang, Y. and Xia, S.B., (2019), "The influence of wetland media in improving the performance of pollutant removal in water treatment: A review", *Appl. Ecology Environ. Res.,* **17**(2), 3803-3818. http://dx.doi.org/10.15666/aeer/1702_38033818.

Xiao, X. (2012), "Preparation of Biomass Sponge-Based Activated Carbon Fiber", Ph.D. Dissertation, Wuhan University of Technology.